Host macrophage response to injectable hydrogels derived from ECM and α-helical peptides

Authors

Nazia Mehrban[a,b*], Catalina Pineda Molina[a,c], Lina M. Quijano[a,c], James Bowen[d], Scott A. Johnson[a,c], Joseph Bartolacci[a,e], Jordan T. Chang[a], David A. Scott[f], Derek N. Woolfson[f,g,h], Martin A. Birchall[b], Stephen F. Badylak[a,c,e]

[a]McGowan Institute for Regenerative Medicine, University of Pittsburgh, 450 Technology Drive, Suite 300, Pittsburgh, PA 15219-3110, USA, [b]UCL Ear Institute, University College London, 332 Grays Inn Rd, London, WC1X 8EE, UK, [c]Department of Surgery, School of Medicine, University of Pittsburgh, University of Pittsburgh Medical Center Presbyterian Hospital, 200 Lothrop Street, Pittsburgh, PA 15213, USA, [d]School of Engineering & Innovation, The Open University, Walton Hall, Milton Keynes, MK7 6AA, UK, [e]Department of Bioengineering, University of Pittsburgh, 3700 O'Hara Street, Pittsburgh, PA, 15261, USA, [f]School of Chemistry, University of Bristol, Cantock's Close, Bristol, BS8 1TS, UK, [g]School of Biochemistry, University of Bristol, University Walk, Bristol, BS8 1TD, UK, [h]Bristol BioDesign Institute, University of Bristol, 24 Tyndall Avenue, Bristol, BS8 1TQ, UK

∗Corresponding author. N. Mehrban (e-mail: n.mehrban@ucl.ac.uk); Permanent Address: UCL Ear Institute, University College London, 332 Grays Inn Rd, London, WC1X 8EE, UK; +44 (0) 203 456 7870.

Abstract

Tissue engineering materials play a key role in how closely the complex architectural and functional characteristics of native healthy tissue can be replicated. Traditional natural and synthetic materials are superseded by bespoke materials that cross the boundary between these two categories. Here we present hydrogels that are derived from decellularised extracellular matrix and those that are synthesised from *de novo* α-helical peptides. We assess *in vitro* activation of murine macrophages to our hydrogels and whether these gels induce an M1-like or M2-like phenotype. This was followed by the *in vivo* immune macrophage response to hydrogels injected into rat partial-thickness abdominal wall defects. Over 28 days we observe an increase in mononuclear cell infiltration at the hydrogel-tissue interface without promoting a foreign body reaction and see no evidence of hydrogel encapsulation or formation of multinucleate giant cells. We also note an upregulation of myogenic differentiation markers and the expression of anti-inflammatory markers Arginase1, IL-10, and CD206, indicating pro-remodelling for all injected hydrogels. Furthermore, all hydrogels promote an anti-inflammatory environment after an initial spike in the pro-inflammatory phenotype. No difference between the injected site and the healthy tissue is observed after 28 days, indicating full integration. These materials offer great potential for future applications in regenerative medicine and towards unmet clinical needs.

Keywords: hydrogels; biomaterials; peptide; ECM; macrophage

1. Introduction

The repair or replacement of damaged tissue using tissue engineering strategies is strongly influenced by the material selected to mimic the architecture and functional characteristics of native healthy tissue. Published sources of bespoke materials are either biologically derived or synthetic.[1, 2] *In vitro* response to these biomaterials is usually assessed by their ability to promote specific cell responses. However, it is the host immune response to implanted biomaterials that is the critical, if not the defining, determinant of clinical success or failure.[3, 4] A desirable host response relies on cell infiltration and material integration/ remodelling in support of an optimal functional outcome. Prolonged inflammation typically results in the formation of granulation tissue or fibrous capsules,[5] seroma, scars and encapsulation.[6] Such an effect results in the isolation of the implanted material from the surrounding healthy tissue and prevents the formation of new functional tissue. Macrophages represent a major cellular component of the innate immune response to biomaterials. These cells show diverse plasticity in their functions ranging from pro-inflammatory to anti-inflammatory and reparative phenotypes.[7, 8] Contrary to accepted 25-year dogma, macrophages, among other cell types such as muscle-specific regulatory T cells and satellite cells,[9] are essential for normal tissue development.[10-13] Macrophages are necessary for successful tissue and organ regeneration in regenerative species such as the axolotl,[14, 15] and have the ability to affect stem cell/ progenitor cell differentiation,[16] and proliferation (i.e., are not necessarily “end stage” cells).[17] Given this relatively recent understanding of macrophage biology and their role in critical life processes, the signalling molecules, physical factors, and environmental factors that influence macrophage phenotype are of great interest to the biomaterials community.

Naturally occurring biomaterials composed of extracellular matrix (ECM), such as decellularised tissues[18-20], have been shown to contain a variety of potent signalling molecules that are released or exposed during degradation of the matrix. These include cryptic peptides,[14] cytokines and

chemokines,[20, 21] and, most recently, embedded matrix bound nanovesicles (MBV).[22] In addition to the chemical cues, these materials provide physical signals such as material stiffness, pore size, and load transfer,[20] which have all been shown to influence macrophage phenotype.[23] Several tissue types have been decellularised and used either in their original form, as sheets[24], or as injectable hydrogels.[20] The tissues used include dermis,[25, 26] small intestinal submucosa (SIS),[27-29] urinary bladder matrix (UBM),[30, 31] liver,[32] tendons,[33] and whole limbs[34]. The use of decellularised ECM in clinical applications is commonplace with several FDA-approved ECM products currently available on the market including AlloDerm®, NeoForm™, GraftJacket®, Strattice™, Meso BioMatrix®, SynerGraft® Oasis® and Surgisis®.

There have been many attempts to mimic properties of the native ECM within synthetic biomaterials.[35-37] It is possible to study individual ECM proteins and to design peptides that are capable of hydrogel configurations.[38-42] Some aspects of the complexity of naturally occurring ECM can be incorporated through the addition of cell-guiding chemical moieties.[43-45] The use of synthetic peptides to accomplish these ends is not new, and there are several reports of natural proteins that are used to create hydrogels suitable for clinical applications.[46-48] The benefits of the previously described hydrogelating self-assembling fibre (hSAF) system include their stable α-helical structure, modifiable chemistry and ability to form at low concentrations compared to other peptide-based systems.[42, 43, 49] Briefly, the hSAF system is formed from two complementary *de novo* designed α-helical peptides. The two peptide sequences form sticky-ended dimers that assemble end-to-end to form fibres. At mM concentrations, the mixed hSAF peptide fibres form self-supporting hydrogels. Combined with added chemical functionality, such as the addition of adhesive ligands, these gels offer at least partial control over cell adhesion, migration and differentiation[43], all characteristics of a material with high clinical translational potential.

While there are clear compositional differences between SIS, UBM and hSAFs, they all form hydrogels with fibrous networks through which cells can migrate and form three-dimensional constructs. Herein, we investigate the macrophage response to injectable UBM, SIS, bovine collagen (type I; FibriCol) and hSAF hydrogels in a partial thickness abdominal wall defect model in Sprague Dawley rats over 28 days, using the native tissue for comparison. Macrophage interaction with these materials will provide a pre-clinical indicator of the likely cell response *in vivo* and offer insights into strategies for promoting cell infiltration and functional restoration of damaged tissue.

2. Materials and Methods

2.1 Material Preparation

2.1.1 Small Intestinal Submucosa

Porcine small intestinal submucosa (SIS) was prepared using previously described methods [50]. Briefly, the intestine was flushed with double distilled water, opened horizontally and most of the tunica mucosa, and entirety of tunica serosa and tunica muscularis externa were removed using a scraper. The remaining tunica submucosa and basilar layers of the tunica mucosa were cut to 80 g particles and shaken at 300 rpm for 2 hrs at room temperature in 0.1% peracetic acid (v/v) (Rochester Midland, USA) with 4% ethanol (v/v) (Decon Laboratories, USA) in Type I H_2O. Tissue was washed thrice in Phosphate Buffered Saline (PBS; Fisher Scientific, USA) and sterile water and shaken at 300 rpm for 15 mins each before being frozen overnight at -20°C, cut into 1 cm x 1 cm sections, lyophilised and milled using a 60 µm mesh on a Wiley Mill (GE Motors & Industrial Systems, USA). Milled small intestinal submucosa (SIS) was stored at room temperature and in the dark until required.

2.1.2 Urinary Bladder Matrix

Urinary bladders were harvested from market-weight (N240 lbs.) pigs (Animal Biotech Industries, USA). The bladders were decellularised as previously described [51]. Briefly, they were rinsed using double distilled water and the urethra and ureter removed. The bladders were opened along their length and a bevelled scraper was used to stretch the muscle across the abluminal surface of the tissue. The tunica serosa, tunica muscularis externa, tunica submucosa and muscularis mucosa were gently removed by making a shallow incision along the length of the bladder (from the apex to the neck). The remaining tunica propria and basement membrane were submerged in double distilled water to reveal any remnant muscle fibres. These remaining fibres were removed and the urinary bladder matrix (UBM) was cut to 80 g particles and shaken at 300 rpm for 2 hrs at room temperature in 0.1% peracetic acid (v/v) with 4% ethanol (v/v) in Type I H_2O. The UBM was then washed thrice in PBS and sterile water on an orbital shaker at 300 rpm for 15 mins each before being frozen overnight at -20°C, cut into 1 cm x 1 cm sections, lyophilised and milled using a 60 µm mesh on a Wiley Mill. Milled UBM was stored at room temperature and in the dark until required.

2.1.3 hSAF Peptides

Two complementary peptides (hSAF-p1 and hSAF-p2) were synthesised as previously described.[49] Briefly, the peptides were synthesised on a 0.1 mmol scale by solid phase peptide synthesis on a CEM "Liberty Blue" microwave-assisted peptide synthesiser (CEM, USA) using fluorenylmethyloxycarbonyl (Fmoc) chemistry. After cleavage from the resin, the peptides were purified by reverse-phase HPLC (Jasco, UK) on a Luna C18 column (5 µm, 100 Å, 4.6 mm x 150 mm ID), and their masses confirmed by MALDI-TOF mass spectrometry (Applied Biosystems 4700 Proteomics MALDI-TOF Analyzer). Peptides were then lyophilised and stored under air at 4°C until required.

2.2 Hydrogel Preparation

For SIS and UBM the lyophilised powders were first digested using 1 mg/mL pepsin (Sigma, USA) in 0.01 N HCl for 48 hrs at room temperature whilst continuously stirring. Digested SIS and UBM were neutralised using 0.1 N NaOH and PBS to concentrations of 8 mg/mL (SIS) and 15 mg/mL (UBM). Collagen hydrogels (FibriCol, Advanced Biomatrix, USA) were formed according to manufacturer's instructions to a concentration of 8 mg/mL. 1 mM hSAF hydrogels were produced using previously described methods.[43]

2.3 Bone Marrow-derived Macrophage Isolation and Culture

Bone marrow-derived mononuclear cells were obtained from female C57bl/6 mice (Jackson Laboratories, USA) and differentiated into macrophages using a previously described technique [29]. In brief, the femur and tibia were isolated and washed in supplemented Dulbecco's Modified Eagle's Medium (S-DMEM) containing DMEM high glucose (Gibco, USA), supplemented with 10% fetal bovine serum (FBS) (Invitrogen, Carlsbad, USA), 10% L929 cell supernatant, 50 mM beta-mercaptoethanol (Gibco, USA), 100 U/mL penicillin, 100 µg/mL streptomycin, 10 mM non-essential amino acids (Gibco, USA), and 10 mM Hepes buffer. After removing the ends of each bone, the marrow was flushed using a 30-gauge syringe needle filled with S-DMEM. Cells were then centrifuged at 1500 g for 5 mins before filtering through a 70 µm cell filter.

The effect of the hydrogels on the differentiation of monocytes into macrophages was evaluated and compared with differentiated cells cultured on tissue culture plastic. 24-well plates previously coated with one of the test hydrogels (1 mM hSAF, 8 mg/mL collagen, 8 mg/mL SIS, and 15 mg/mL UBM to match stiffnesses between the hydrogels to 1 kPa; **Figure S1**) [42, 52, 53] or uncoated controls were seeded with 1 x 10^6 cells per well in S-DMEM and were incubated at 37°C, 5% CO_2 and 100% relative humidity and the media changed every 48 hrs.

2.4 Macrophage Activation and Immunolabeling

After 7 days of differentiation the expression of macrophage activation markers was evaluated on macrophages seeded on the hydrogel coated plates and uncoated tissue culture plastic controls. As controls of macrophage activation, 100 ng/mL LPS (Sigma Aldrich, USA) and 20 ng/mL IFN-γ (Peprotech, USA) to induce M1 macrophage activation, 20 ng/mL IL-4 to induce M2 macrophage activation were used. After 24 hrs of induced activation the cells were washed with PBS and fixed for 1 hr with 2 % paraformaldehyde (Fisher Scientific, USA) (500 µL on tissue culture plastic, 1 mL for hydrogels; and 700 µL for tissue culture plastic control samples). The cells in all wells (hydrogel and tissue culture plastic controls) were then washed three times with PBS before 1x blocking buffer was added (1 mL for hydrogels/ 500 µL for uncoated samples) and the samples incubated at room temperature for 1 hr. After removing the blocking buffer, 500 µL of the primary antibody (monoclonal rat anti- murine F4/80 (CI-A3-1) (Novus Biologicals, USA), rabbit anti-murine Fizz1 (RELMa; Peprotech, USA), polyclonal rabbit anti-iNOS (Novus Biologicals, USA) and polyclonal rabbit anti-liver Arginase1 (Abcam, USA) was added (1:100 in blocking buffer for each) and incubated overnight at 4°C. The following day, the primary antibody was removed and the samples washed twice with PBS before 500 µL of the Alexa Fluor 488-conjugated secondary antibody (Invitrogen, USA) was added to each well (1:200 in blocking buffer goat anti-rat for F4/80 and goat anti-rabbit for iNOS, Fizz and Arginase1 and the samples incubated at room temperature in the dark for 1 hr. After incubation the samples were washed twice with PBS before the cell nuclei were counterstained with 500 µL 4' 6-diamidino-2-phenylindole (DAPI; 500 nM in type I water) (Sigma Aldrich, USA) and incubated in the dark at room temperature for 5 mins. The samples were washed again with PBS and left in fresh PBS before they were imaged blindly. Images of three 200X fields were taken for each of the three wells (for each condition) using an inverted live-cell microscope (Zeiss, USA), standardising the light exposure times based on those set for cytokine-treated macrophages. The percent of positive cells for each marker was quantified using CellProfiler Image Analysis Software (http://www.cellprofiler.org), positive macrophages (green label) were identified by their co-localisation

with DAPI positive nuclei. The percent of expressing macrophages was then determined by dividing the identified positive cells by the total number of macrophage nuclei. Three biologic replicates were evaluated, and three images were analysed for each marker per replicate.

2.5 In Vivo Studies of SIS, UBM, hSAF and Collagen

All animal experiments were conducted in accordance with the NIH Care and Use of Laboratory Animals guidelines. Female Sprague-Dawley rats (~250 g; Envigo, USA) were anaesthetised using 2-3% isofluorane (Baxter, USA) and their abdominal area shaved. They were then sterilised using 70% ethanol and Betadine solution (Purdue Pharma, USA). A midline skin incision was made on the abdominal wall to expose the abdominal muscles (**Figure 1**). 1 cm^2 bilateral partial thickness abdominal wall defects were created by removing the internal and external oblique muscles and retaining the transversalis fascia and peritoneum. Defects were marked at the border with four-point sutures using non-degradable polypropylene sutures (Med-Vet International, USA). Defects were then injected with 150 µL of the hydrogel solution being tested. Gel concentrations were determined from rheological studies to ensure a similar stiffness of material, 1 kPa, was used for the *in vivo* studies (**Figure S1**). [42, 52, 53] Collagen (FibriCol, Advanced BioMatrix, USA) was prepared according to manufacturing protocols to produce a final concentration of 8 mg/mL. For hSAF hydrogels 2 mM hSAF-p2 in 3-(*N*-morpholino) propanesulfonic acid (MOPS)-buffer (20 mM MOPS, 5 mM sodium acetate, 1 mM EDTA (Fisher Scientific, USA) pH 7.4 was added to a syringe containing 2 mM hSAF-p1 immediately before injection at a total gel concentration of 1 mM. All materials were gelled *in situ* based on gelation times determined from the rheological studies (**Figure S1C**) before the wound was closed using vicryl sutures (Medsurplus online, USA). Two types of controls were used for this study; abdominal wall with no injury and abdominal wall with defect to match the time points of the study but with no material injected.

Post-surgery the animals were given a daily dose of 0.05 mg/kg buprenorphine hydrochloride (Buprenex) (Covetrus, USA) by subcutaneous injection and 5 mg enrofloxacin (Baytril (Bio-Serv, USA)) orally for the first three days. The tissue at the injection site was explanted at 1 day, 3 days, 7 days, 14 days or 28 days after surgery (N=3 for each time point). Samples were excised using 8 mm punch biopsies and fixed in either 2.5% glutaraldehyde (for scanning electron microscopy) or 10% Neutral Buffered Formalin (NBF; for histology and fluorescent microscopy (VWR, USA) or frozen in liquid nitrogen and stored at -80°C for polymerase chain reaction (PCR).

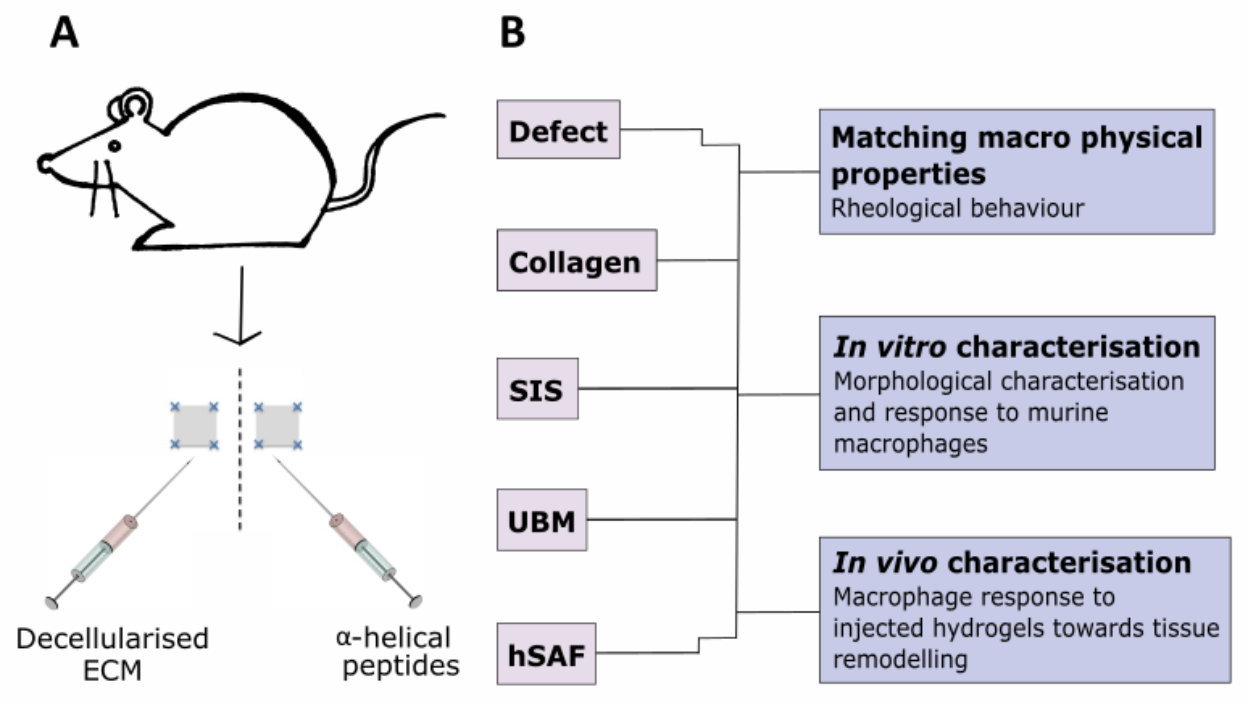

Figure 1: Cartoon representation of the surgical model and study outline. (A) Bilateral partial thickness defects were created on the abdominal wall of female Sprague-Dawley rats measuring 1 cm by 1 cm. (B) The three-part study consisted of matching macro physical properties, *in vitro* characterisation and *in vivo* characterisation of the defect (wound alone with no hydrogel injected), collagen hydrogels, SIS hydrogels (small intestinal submucosa), UBM hydrogels (urinary bladder matrix) and hSAF hydrogels (hydrogelating self-assembling peptides).

2.6 Scanning Electron Microscopy

Three samples for each condition were fixed in 2.5% glutaraldehyde for 1 hr and triple washed in PBS for 15 mins each. They were then dehydrated in graded ethanol (30%, 50%, 70%, 90% and 100% v/v in distilled H_2O) for 15 mins each and critical point dried at 50 bar. The dried samples were then sputter coated with 5 nm of gold-palladium and imaged using a JEM-6335F scanning electron microscope (Jeol, USA) at a working distance of 8 mm and magnifications of 25X, 200X, 1000X and 5000X.

2.7 Histology

The NBF samples were embedded in paraffin, cut into 5 µm thick sections, and mounted onto glass slides. Hematoxylin and eosin (H&E; Sigma-Aldrich, USA) staining was performed following manufacturer's instructions, and after deparaffinisation using xylene and graded series of ethanol solutions (100%, 95%, 75%). Stained slides were dehydrated using a graded series of ethanol solutions (75%, 95%, 100%) prior to cover-slipping. Three biologic replicates with three different images were taken from each sample at the gel-tissue interface. A total of nine images were analysed per group and time point at 200X magnification.

2.8 Immunolabeling of Explants

5 µm sections of the explanted tissues were cut and mounted onto slides in paraffin. Deparaffinisation was performed by dipping the slides in xylene (Fisher Scientific, USA) three times for 3 mins each, which was followed by one min washes in 100 % ethanol, 95 % ethanol (in type I water) and 70 % ethanol. The slides were then rinsed under running tap water for 2 mins before they were placed in 10 mM antigen retrieval buffer at 95-100°C for 20 mins. The samples were cooled on ice to 35°C and washed twice in TRIS

buffered saline/Tween 20 buffer (Sigma Aldrich, USA) for 3 mins each. After two washes in PBS for 3 mins each, the slides were dried and incubated in 1x blocking buffer at room temperature for 1 hr in a humidified chamber to inhibit non-specific binding. After incubation with the blocking buffer the slides were incubated overnight in the primary antibody (a triple stain of rabbit anti-human CD86 (clone EP1158Y, Abcam, USA; an M1-phenotype marker) and mouse anti-rat CD68 (clone ED1, Abd Serotec, USA; a macrophage marker) 1:150 in blocking buffer and goat anti-human CD206, polyclonal, (R&D systems, USA; an M2-phenotype marker) 1:100 in blocking buffer) at 4°C.

The following day the primary antibody was removed, slides washed three times in PBS for 3 mins each and secondary antibodies were added: donkey anti-mouse Alexa Fluor-594 (1:200 dilution, Invitrogen, USA), donkey anti-rabbit PerCPCy5.5 (1:300 dilution, Santa Cruz, USA), and donkey anti-goat Alexa Fluor-488 (1:200 dilution, Invitrogen, USA) and incubated in a dark humidified chamber for 1 hr at room temperature. Slides were washed three times in PBS for 3 mins each, cell nuclei stained using 500 nM DAPI in type I water for 5 mins, dipped in type I water for a final wash and mounted with DAKO Mounting Media (Carpinteria, USA) before covering with a cover slip. Three multispectral epifluorescent images were acquired for each of the three biological replicates at the mesh-tissue interface (Nuance Multispectral Imaging System, CRi Inc., USA) at 200X magnification.

Macrophages were defined as CD68 positive co-localised with nuclei. The total number of cells co-expressing CD68 with CD86 and/or CD206 was quantified for each image using CellProfiler Image Analysis Software (http://www.cellprofiler.org). The M1-like subpopulation was calculated by subtracting the number of triple-labelled $CD68^{+}CD206^{+}CD86^{+}$cells from the $CD68^{+}CD86^{+}$cells, to avoid duplicating cell counts. Similarly, the M2-like subpopulation of macrophages was calculated by subtracting the number of triple-labelled $CD68^{+}CD206^{+}CD86^{+}$cells from the $CD68^{+}CD206^{+}$cells. A ratio of the number of M2-like to M1-like cells was calculated for each field by dividing the number of M2-like macrophages by the number of M1-like macrophages.

2.9 Polymerase Chain Reaction

Total RNA was extracted from tissue sections (three biological replicates and three technical replicates for each sample) by homogenising the samples with 1000 µL TRIzol reagent (Ambion, USA) using TissueRuptor disposable probes (Qiagen, USA) 800 µl of each of the homogenised samples was mixed with 200 µL chloroform, vortexed for 15 secs and centrifuged at 12,000 g for 10 mins. The aqueous phase was then transferred to a new tube and the RNA precipitated with 3M sodium acetate (1/10 of the volume; Novagen, USA) and isopropanol (1 volume; Fisher Scientific, USA), followed by centrifugation at 18,000 g for 20 mins. The extracted RNA was purified by washing the pellet in 75% ethanol with an additional centrifugation at 18,000 g for 15 mins. The RNA pellet was air-dried and resuspended in nuclease-free water. 1 mg of RNA was converted to cDNA using a High Capacity cDNA Reverse Transcription Kit (Applied Biosystems, USA) according to manufacturer instructions. Real-time quantitative polymerase chain reaction (qPCR) was conducted using PowerUp™ SYBR® Green Master Mix (Applied Biosystems, USA) to determine the expression levels of different macrophage activation markers (TNF-α, IL-1β, IL-10, and Arginase1) and mononuclear signals of myogenesis (MyF5, MEF2, Myogenin, and MHC) **Table 1**. The levels of expression were normalised against the housekeeping gene GAPDH. Results were expressed as Log(2) of fold change ($2^{-\Delta\Delta Ct}$) relative to native muscle.

Table 1: Primer sequences

TNF-α	F: 5´-ATACACTGGCCCGAGGCAAC-3´
	R: 5´-CCACATCTCGGATCATGCTTTC-3´
IL-1β	F: 5´-CTCTGTGACTCGTGGGATGATG-3´

	R: 5´-CACTTGTTGGCTTATGTTCTGTCC-3´
IL-10	F: 5´-CCTTACTGCAGGACTTTAAGGGTTA-3´
	R: 5´-TTTCTGGGCCATGGTTCTCT-3´
Arginase1	F: 5´-CATATCTGCCAAGGACATCG-3´
	R: 5´-GGTCTCTTCCATCACTTTGC-3´
MHC	F: 5´-TGACTTCTGGCAAAATGCAG-3´
	R: 5´-CCAAAGCGAGAGGAGTTGTC-3´
MyF5	F: 5´-GAAGGGAAGACAAGCAGCAC-3´
	R: 5´-GCAAAAAGAACAGGCAGAGG-3´
Myogenin	F: 5´-CAGTGAATGCAACTCCCACA-3´
	R: 5´-CAAATGATCTCCTGGGTTGG-3´
MEF2	F: 5´-TGCTGCTCTCACTGTCACTAC-3´
	R: 5´-TTCACGACTTGGGGACACTG -3´
MyoD	F: 5´-CGACTGCCTGTCCAGCATAG-3´
	R: 5´-GGACACTGAGGGGTGGAGTC-3´
GAPDH	F: 5´-GTGGTGCCAAAAGGGTCAT-3´
	R: 5´-ATTTCTCGTGGTTCACACCCA-3´

2.10 Statistical Analysis

All data are presented as “mean ± standard error of mean (SEM)”. The mean value differences between groups, and whether the differences were significant, were determined by either a two-way Analysis of Variance (ANOVA) or a non-parametric ANOVA with a post-hoc Tukey HSD (honestly significant difference) test. The fold change gene expression relative to native muscle was analysed using the BootstRatio Web Application for the ratio between the treatments and the control.[54] The significance level was set at $p < 0.05$.

3.0 Results

3.1 *In Vitro* Effect of ECM-derived and α-Helical Peptide-based Hydrogels on Primary Murine Macrophages

In vitro, the presence of the hydrogels did not inhibit monocyte differentiation into macrophages. As shown in **Figures 2A and 2B**, at least 50% of the cells seeded onto the hSAF, collagen, SIS, and UBM hydrogels were positive for the pan-macrophage marker F4/80, indicating successful differentiation, without significant differences between the different hydrogel types.

In addition to supporting the differentiation of monocytes into macrophages, the presence of the hydrogels induced a spontaneous macrophage activation *in vitro*, as seen by the positive staining of the pro-inflammatory M1-like phenotype marker iNOS, and the anti-inflammatory M2-like phenotype markers (Fizz1, and Arginase1). There were no statistical differences in F4/80, iNOS, Fizz1 and Arginase1 expression between hSAF, collagen, SIS and UBM hydrogels (**Figure 2A and 2B**). However, fluorescent studies showed that the highest expression of both M1-like and M2-like markers was observed in a ‘band’ that formed across all hSAF hydrogels (**Figure 2A**). This band was not visible in any of the other hydrogels studied.

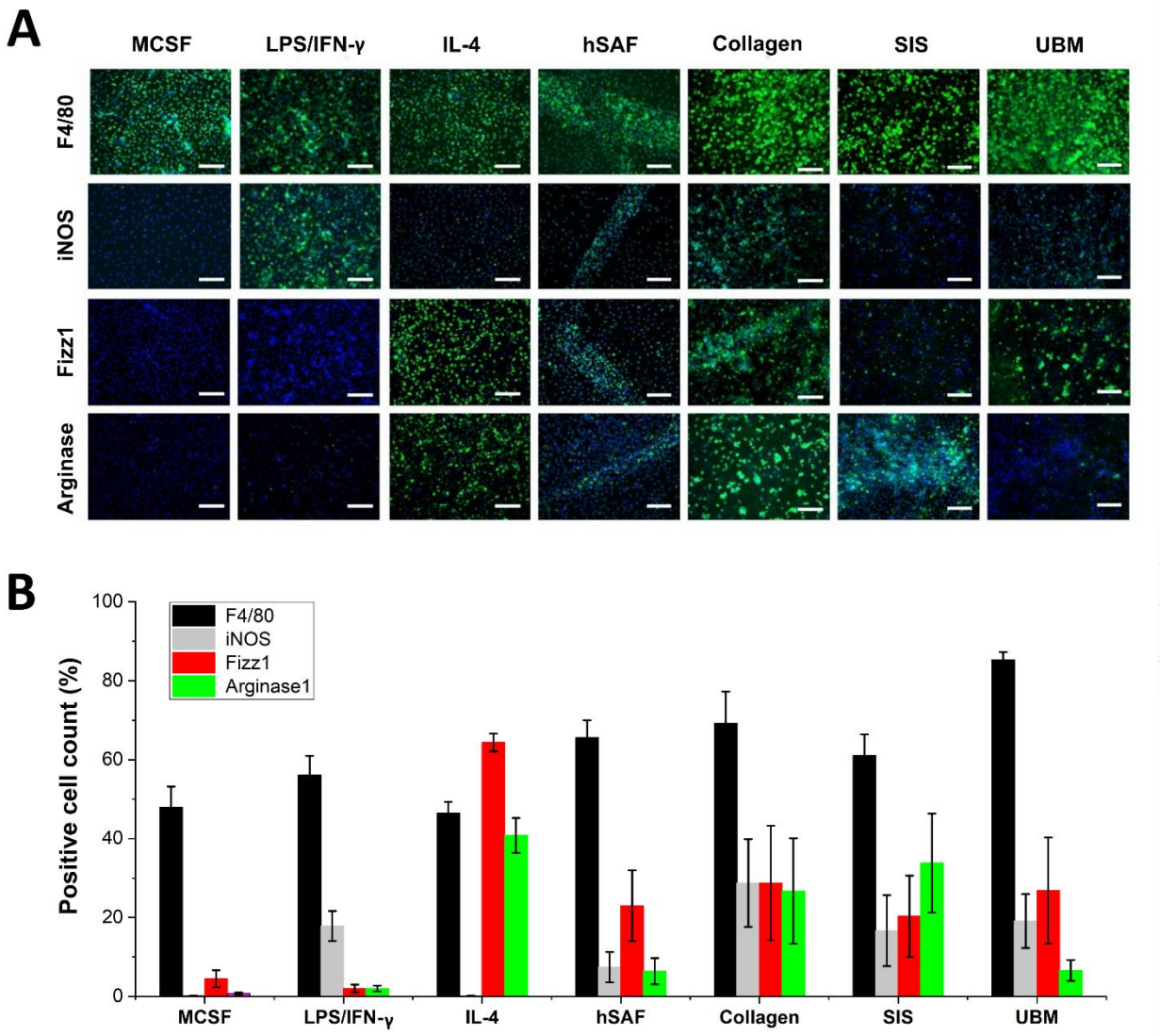

Figure 2: *In vitro* characterisation of hSAF, collagen, SIS and UBM hydrogels. (A) Fluorescence-microscope images of the pan-macrophage marker (F4/80), a marker of activation towards an M1-like (iNOS) or M2-like (Fizz1 and Arginase1) phenotype depicting cell nuclei (blue) and positive macrophage markers (green). (B) Percentage of macrophages expressing F4/80 (black), iNOS (grey), Fizz1 (red) and Arginase1 (green) in comparison to the total number of nuclei in each field of view. N= 3 biological replicates and 3 technical replicates; magnification: 200X; scale bar: 100 µm. No statistically significant differences between the groups were noted ($p < 0.05$).

3.2 Morphological Characterisation of Injected Hydrogels

A rat abdominal wall partial thickness defect model was used to evaluate the host response to implanted collagen, hSAF and ECM hydrogels.[55] There were no discernible morphological differences between the implanted hydrogels and the surrounding healthy tissue after 28 days. (**Figure 3A**). The acute host response, days 1 to 7, to the injected hydrogels was characterised by an increased infiltration of mononuclear cells at the hydrogel-tissue interface that increased over time. There was no encapsulation of the hydrogels or formation of multinucleate giant cells. By day 28 there were no signs of foreign body reaction at the host tissue interface for any of the hydrogels. All injected hydrogels were associated with pro-healing outcomes by day 28. Healing was confirmed through the presence of organised tissue, newly formed ECM and neovascularisation, although muscle fibre formation was not evident at any of the repaired sites (**Figure 3B**).

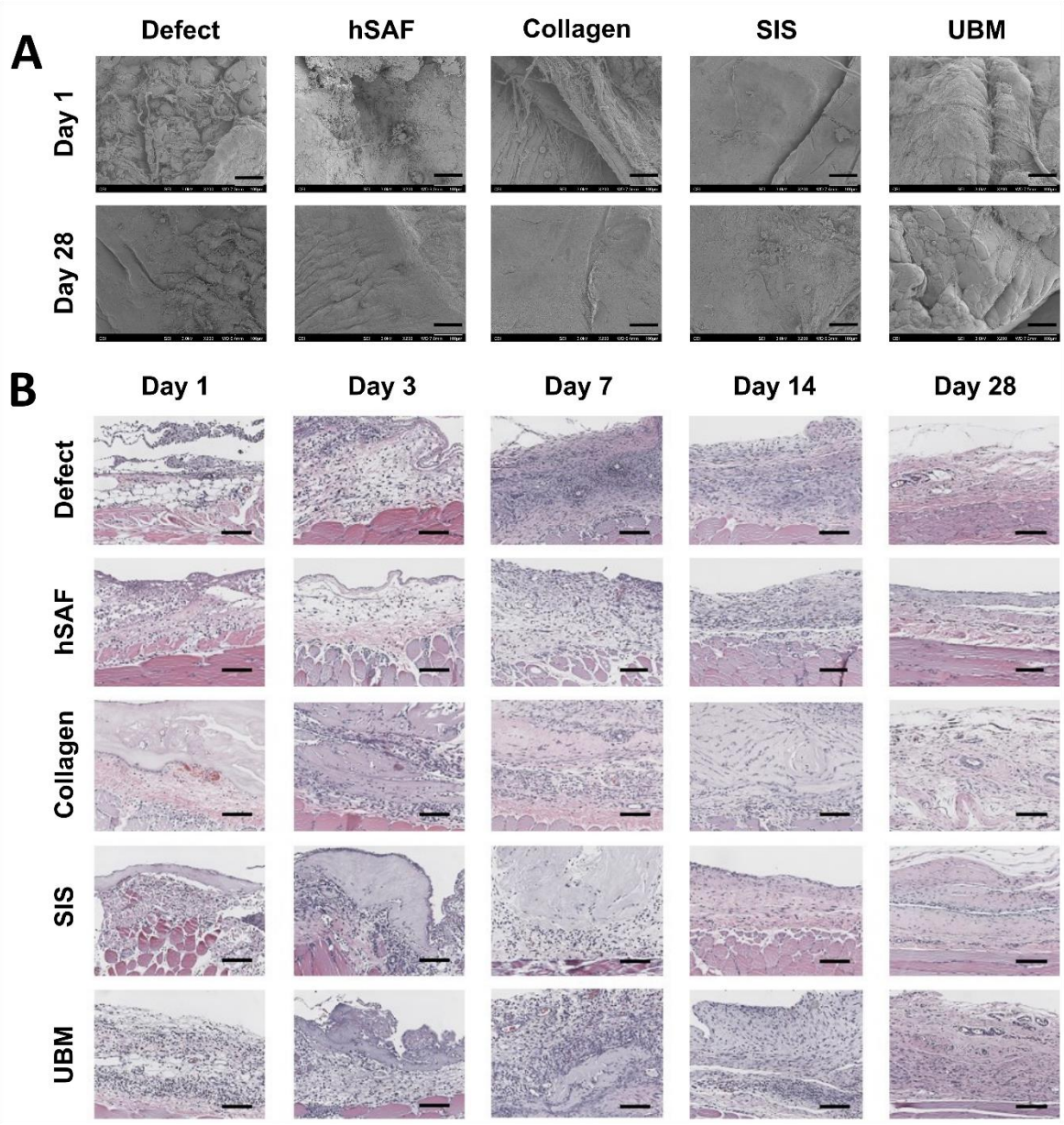

Figure 3: Morphological characterisation of implanted hydrogels. (A) Scanning electron micrographs and (B) histomorphologic characterisation, with haematoxylin (purple) and eosin (pink), of tissue repair at the defect site over 28 days. N= 3 biological replicates and 3 technical replicates; magnification: 200X; scale bar: 100 µm.

Initially, quantification of myogenesis at the wound site showed a decrease in MyF5 expression after day 3 for all hydrogels investigated, indicating a decrease in cell proliferation and an onset of myogenic differentiation (**Figure 4A**). No statistical difference was observed in the MEF2 expression between the hydrogels and the defect over 28 days (**Figure 4B**). However, a decrease in Myogenin expression was noted across all sample types by day 28 although only collagen showed statistical difference to the defect alone (**Figure 4C**); further supporting the histomorphologic findings. Finally, while some increase in the expression of the late myogenic factor, MHC, was observed for all sample types by 28 days, these differences were not statistically significant between the hydrogel types (**Figure 4D**) and indicated that no mature muscle fibre had formed.

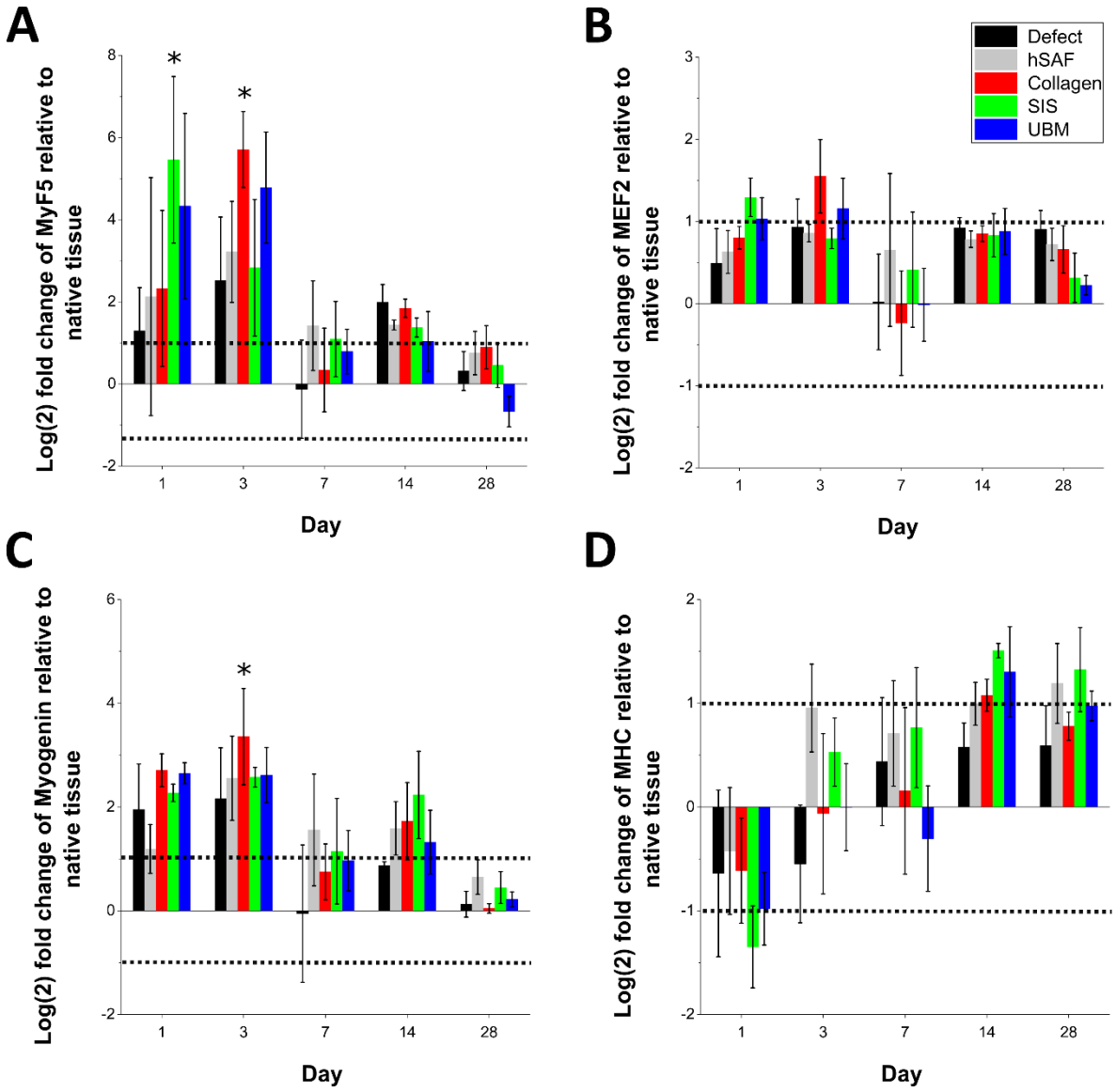

Figure 4: Gene expression of myogenesis markers. Expression of (A) MyF5 (B) MEF2 (C) Myogenin and (D) MHC for defect (black), hSAF (grey), collagen (red), SIS (green) and UBM (blue) over 28 days. N= 3 biological replicates and 3 technical replicates. Dotted lines indicate the biologically significant threshold. * illustrates statistically significant difference between the indicated hydrogel and the native tissue ($p < 0.05$).

3.3 Macrophage Response to Implanted Hydrogels

Macrophage phenotype was determined to evaluate the *in vivo* innate host response to the hydrogels 28 days post-implantation. While fluorescence studies suggested some differences in macrophage marker expression over 28 days, particularly in images obtained for hSAF CD206+ expression on day 7 (**Figure 5A**), quantification showed that the ratio of M2-like phenotype to M1-like phenotype is similar for hSAF, collagen and SIS hydrogels immediately after surgery with all three exhibiting ratios < 0.2 (**Figure 5B**). UBM hydrogels showed an initial spike of the M2-like:M1-like ratio on day 1 post-surgery and again on day 14, although there was no statistical difference in marker expression across hSAF, UBM, SIS and collagen hydrogels by day 28 (**Figure 5B**).

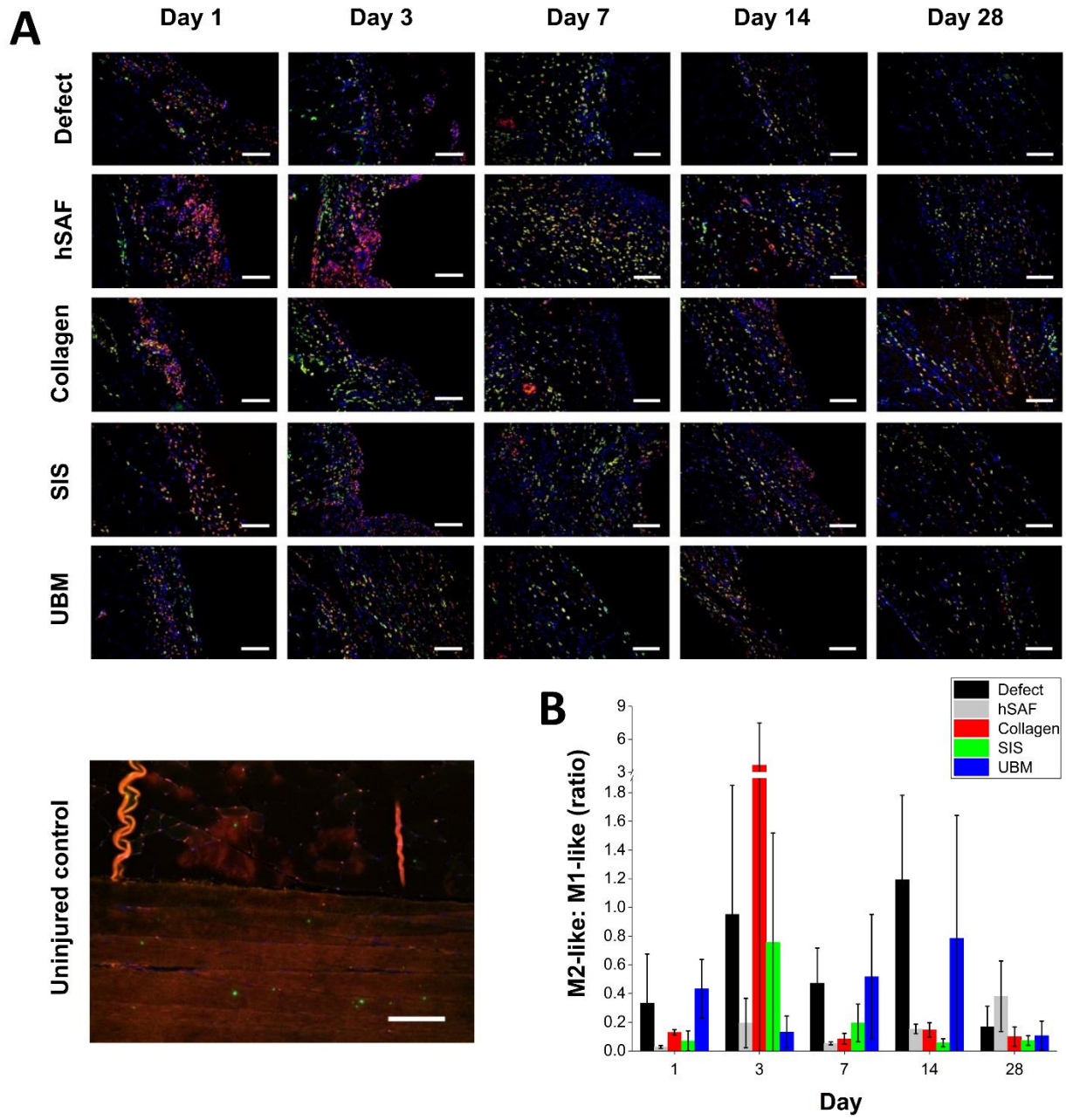

Figure 5: Macrophage response to implanted hydrogels. (A) Fluorescent images of macrophages at the defect site over 28 days depicting either an M1-like (CD86+; orange) or M2-like (CD206+; green) phenotype. Macrophage marker (CD68+; red) and cell nuclei (DAPI; blue) are also shown. (B) Ratio of cells expressing CD86+ and CD206+ over 28 days; defect (black), hSAF (grey), collagen (red), SIS (green) and UBM (blue). N= 3 biological replicates and 3 technical replicates; magnification: 200X; scale bar: 100

μm. No statistically significant differences between the indicated hydrogel and the native tissue were noted ($p < 0.05$).

A more in-depth study of M1-like and M2-like cytokine expression showed that pro-inflammatory cytokines TNFα and IL-1β increased for collagen and UBM hydrogels on day 3 although there was no statistical difference in the expression of the two markers between all gel types and the native tissue by day 28 (**Figure 6A and 6B**). Anti-inflammatory cytokine expression (IL-10) is significantly higher for hSAF, SIS and UBM gels compared to the native tissue at early time points but by day 14 only remains high for hSAF and collagen samples (**Figure 6C**). By day 28 there is no statistically significant difference between the gels and the native tissue. Similarly, although temporary increases in Arginase1 expression were noted for collagen and SIS early in the study, by day 28 there is no difference between the hydrogels and the native tissue (**Figure 6D**).

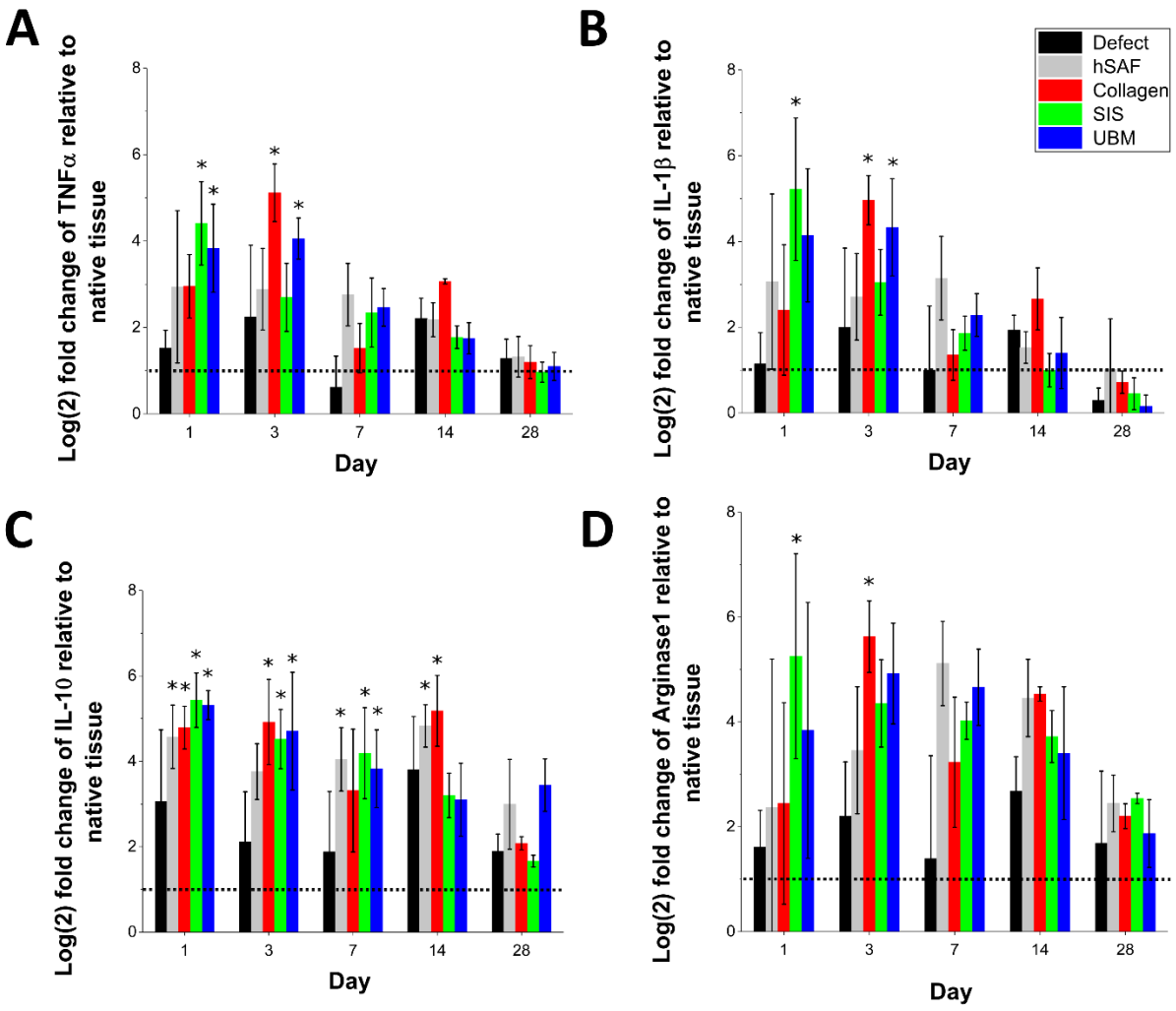

Figure 6: Macrophage response to implanted hydrogels. Macrophage activation showing (A) TNFα (B) IL-1β (C) IL-10 and (D) Arginase1 gene expression for defect (black), hSAF (grey), collagen (red), SIS (green) and UBM (blue). N= 3 biological replicates and 3 technical replicates. Dotted lines indicate the biologically significant threshold. * illustrates statistically significant difference between the indicated hydrogel and the native tissue ($p < 0.05$).

4.0 Discussion

Biomaterials that attempt to mimic the chemical and physical complexity of native tissues provide controllable environments that may actively promote cell attachment and differentiation.[56-59] Hypothetically, these materials are more likely to generate a constructive and functional response *in vivo*, lead to integration with host tissue and minimise the risk of adverse immunological responses. We investigate the macrophage response to complex injectable hydrogels derived from ECM and constructed from *de novo* design peptides. In the former class, UBM-ECM and SIS-ECM have been shown to largely retain the fibrous structure of native tissue and provide the biological signalling potential of the original tissue. [24] In the second, α-helical peptide hydrogels offer a bottom-up design approach with absolute control over hydrogel assembly and structure, and over the cell-guiding chemistry, by adding such cues in known amounts and formulations.[42, 49] Although *in vitro* studies have suggested superiority of all of these hydrogels over commercially available hydrogels,[23, 43, 49, 60] neither class has been investigated *in vivo* in a partial-thickness abdominal model; a model that has been widely used to study foreign body response to biomaterials.[61, 62] Here, we investigate the host inflammatory response to injectable UBM, SIS and hSAF hydrogels over 28 days.

We note that the macrophage response to the hydrogels differs for SIS and UBM compared to other hydrogels: typically, in wound healing a switchover from an M1-like phenotype to an M2-like phenotype should occur by day 7-14. While UBM hydrogels do eventually induce an M2-like phenotype, the delayed changeover may be the result of a slower release of the molecular mediators responsible for this effect. By the end of the study all hydrogel types induced an M2-like phenotype over time, as observed in the *in vitro* macrophage response to the hydrogels.

The chemistries of hSAF and UBM are very different and some of the changes in macrophage behaviour may be attributed to this chemical difference. However, the majority of macrophage marker expression

in hSAF hydrogels, for both M1-like and M2-like phenotypes, is observed across a 'band' that was visible in these particular gel types. We posit that this band is caused by cells contracting the hydrogel and a build-up of tension along areas where the hydrogel remained anchored to the cell culture plate. Although effort was made to ensure experimental protocol was identical for all hydrogels, it has previously been shown that the highly porous hSAF hydrogels not only allow cells to migrate freely through the scaffold but also encourage cell attachment to the fibres[49], which could lead to a build-up of tension in the network. Furthermore, previous studies suggest that substrate stiffness could influence macrophage activation strongly.[63, 64] *In vivo* this tension could induce macrophage activation that could lead to the formation of foreign body giant cells and chronic inflammation or, if controllable, could lead to better tissue remodelling.[64] To test this hypothesis, hSAF gels with different, but controllable, mechanical properties would need to be studied in an *in vivo* model.

Histomorphologic examination of explanted tissues at the injected wound site show no evidence of multinucleate giant cells or a foreign body response previously noted by some researchers in the investigation of polypropylene-based biomaterials in a rat partial thickness abdominal model.[62] Rather, a transition of a pro-inflammatory environment to an anti-inflammatory environment in the hSAF hydrogels is observed. Either the band observed in the *in vitro* studies is not replicated in the *in vivo* studies or the stiffness does not sustain a pro-inflammatory environment over 28 days and possibly is unlikely to have a detrimental effect long-term. An initial infiltration of mononuclear cells, immediately post-injection, was maintained throughout the study and indicates the likelihood of a positive tissue remodelling outcome.[65] This is further supported by the neovascularisation and new ECM observed at the wound site, although no muscle regeneration is observed in any of the explants. Initial signs of myogenesis are noted for all hydrogels, through a decrease in the expression of proliferation markers and an increase in the expression of differentiation markers. This is despite the expression of the late

differentiation complex MHC[66] reaching a plateau between days 14 and 28. Without this terminal differentiation stage mature myofibres cannot develop[67] and a permanent loss of muscle mass could result in compromised functionality. While this is a vital factor in considering tissue remodelling in the abdominal area where the injury was induced and in future studies it may be possible to chemically modify the materials to induce myogenesis, we did not anticipate observing muscle regeneration in the current study as the stiffness of the materials used did not match native muscle stiffness (10 kPa compared to 1 kPa for our hydrogels).[68]

Our studies show that after an initial spike in the M1-like pro-inflammatory phenotype, as expected due to neutrophil and macrophage influx immediately post-injury,[69] all of the injected hydrogels induce an M2-like anti-inflammatory phenotype after 28 days. Though no difference in M2:M1 ratio was noted across the hydrogels, hSAF hydrogels exhibit the highest levels of M2 cytokine expression. A high M2 cytokine expression is an indicator of constructive tissue remodelling and likely to lead to better functional outcomes with a low likelihood of scarring.[64, 69]

Our initial observations on the chemical and physical heterogeneity within UBM, and possibly decellularisation of tissues in general, as well as tensile forces eliciting, and maintaining a possible M1-like phenotype, are not reflected in the *in vivo* studies. Previous research has shown that, *in vivo*, when pro-inflammation is caused specifically by cell debris trapped in an unsuccessfully decellularised scaffold, it is in fact dose-dependent.[6] Similarly, the band observed across hSAF-based macrophage studies is in contact with tissue culture plastic as well as cells. The 3-dimensional environment of an *in vivo* model and exposure to multiple cell types already introduces variables that cannot be replicated in *in vitro* studies. None of the explants excised from the rats that are initially injected with hSAF hydrogels display such

bands or any sign of tension-based cell alignment and differentiation. These observations highlight the limitations of comparing *in vitro* data with *in vivo* results.

Studies conducted specifically on explants show that all of the hydrogels exhibited an M1-like to M2-like transition, generating a pro-healing environment after 28 days, although further tests are required to determine the mechanism by which the materials initiate this transition as well as an investigation of other cell types that play critical roles in muscle development, such as T cells and quiescent satellite cells.[9] While differences between the composition and behaviour of SIS and UBM were noted, the *in vivo* macrophage response remains favourable. As derivatives of healthy tissue, it could be argued that the positive outcome to the injectable form of the matrices is to be expected. However, it has been shown that the considerable chemical and physical modification of the original tissue that has been employed in this study not only allow the complex cell-guiding proteins to be retained but that the manipulation of the materials towards injectable hydrogels introduces superior control over geometry. Similarly, hSAF hydrogels, although far simpler in composition than the ECM hydrogels, have been shown to offer comparable results to their complex counterparts. For the regenerative medicine field, the unparalleled and highly controllable chemical and physical properties offered by hSAF materials could end some of the limitations of existing injectable biomaterials and reduce the probability of chronic inflammation. Although the cell response to both the ECM and synthetic hydrogels, and tissue remodelling abilities, are the primary focus of the present study, these materials may also be used in cell or drug delivery, particularly as further rheological studies could offer valuable insights into controlling the stiffness of the materials. We suggest that multi-purpose, highly tunable biomaterials, such as those investigated here, could be considered in the drive towards regenerative biomaterials for unmet clinical needs.

5.0 Conclusion

Hydrogels derived from decellularised extracellular matrix and synthesised *de novo* designed α-helical peptides have been injected into rat partial thickness abdominal wall defects to examine the immune macrophage response *in vivo*. Over 28 days a progressive increase in mononuclear cell infiltration is observed with no foreign body reaction at the hydrogel-tissue interface, no evidence of hydrogel encapsulation or formation of multinucleate giant cells. Furthermore, the upregulation of myogenic differentiation markers and the expression of anti-inflammatory (M2-like) markers Arginase 1, IL-10, and CD206, indicate pro-remodelling for all injected hydrogels. All hydrogels induce a stable anti-inflammatory environment. No difference between the injected site and the healthy tissue is observed after 28 days, which is indicative of full integration and is promising for future applications as part of regenerative therapeutic approaches to unmet clinical needs.

Data Availability

The raw/processed data required to reproduce these findings cannot be shared at this time due to technical or time limitations.

Declaration of Competing Interest

The authors declare no conflict of interest.

Acknowledgments

This research was supported by The Royal Free Charity (Royal Free Charity Fund 190). N.M. was supported by the Engineering and Physical Sciences Research Council (EP/R02961X/1). D.A.S was supported by the BBSRC South West Biosciences Doctoral Training Partnership (BB/J014400/1 and BB/M009122/1). D.N.W. held a Royal Society Wolfson Research Merit Award (WM140008). The funders had no role in study design;

in the collection, analysis and interpretation of data; in the writing of the report; and in the decision to submit the article for publication. The authors are grateful to Dr. Velankar for access to rheometry equipment, the histology unit at the McGowan Institute for Regenerative Medicine and the University of Pittsburgh Centre for Biologic Imaging. The authors would also like to thank the Gray family for their donations to this research.

CRediT Author Statement

Nazia Mehrban: Conceptualization; Data curation; Formal analysis; Investigation; Methodology; Project administration; Validation; Visualization; Roles/Writing - original draft; Writing - review & editing. **Catalina Pineda Molina**: Conceptualization; Data curation; Formal analysis; Investigation; Methodology; Project administration; Validation; Visualization; Roles/Writing - original draft; Writing - review & editing. **Lina M. Quijano**: Data curation; Investigation; Methodology; Validation; Visualization; Roles/Writing - original draft; Writing - review & editing. **James Bowen**: Conceptualization; Formal analysis; Methodology; Project administration; Roles/Writing - original draft; Writing - review & editing. **Scott A. Johnson**: Conceptualization; Investigation; Methodology; Project administration; Resources; Supervision; Validation; Visualization. **Joseph Bartolacci**: Data curation; Investigation; Methodology; Project administration. **Jordan T. Chang**: Data curation; Investigation; Methodology. **David A. Scott**: Resources; Validation; Writing - review & editing. **Derek N. Woolfson**: Funding acquisition; Resources; Writing - review & editing. **Martin A. Birchall**: Conceptualization; Funding acquisition; Resources; Supervision; Writing - review & editing. **Stephen F. Badylak**: Conceptualization; Methodology; Project administration; Resources; Supervision; Validation; Roles/Writing - original draft; Writing - review & editing.

References

[1] F. Khan, M. Tanaka, Designing smart biomaterials for tissue engineering, International Journal of Molecular Sciences 19 (2018) 1-14.
[2] K. Christman, Biomaterials for tissue repair, Science 363 (2019) 340-341.
[3] S. Franz, S. Rammelt, D. Scharnweber, J. Simon, Immune responses to implants - a review of the implications for the design of immunomodulatory biomaterials, Biomaterials 32 (2011) 6692-6709.
[4] E. Mariani, G. Lisignoli, R. Borzì, L. Pulsatelli, Biomaterials: Foreign Bodies or Tuners for the Immune Response?, International Journal of Molecular Sciences 20 (2019) 636-678.
[5] Z. Sheikh, P. Brooks, O. Barzilay, N. Fine, M. Glogauer, Macrophages, foreign body giant cells and their response to implantable biomaterials, Materials (Basel) 8 (2015) 5671-5701.
[6] R. Londono, J. Dziki, E. Haljasmaa, N. Turner, C. Leifer, S. Badylak, The effect of cell debris within biologic scaffolds upon the macrophage response, Journal of Biomedical Materials Research Part A 105 (2017) 2109-2118.
[7] A. Das, M. Sinha, S. Datta, M. Abas, S. Chaffee, C. Sen, S. Roy, Monocyte and Macrophage Plasticity in Tissue Repair and Regeneration, The American Journal of Pathology 185 (2015) 2596-2606.
[8] L. Parisi, E. Gini, D. Baci, M. Tremolati, M. Fanuli, B. Bassani, G. Farronato, A. Bruno, L. Mortara, Macrophage Polarization in Chronic Inflammatory Diseases: Killers or Builders?, Journal of Immunology Research 2018 (2018) 1-25.
[9] D. Burzyn, W. Kuswanto, D. Kolodin, J. Shadrach, M. Cerletti, Y. Jang, E. Sefik, T. Tan, A. Wagers, C. Benoist, D. Mathis, A Special Population of Regulatory T Cells Potentiates Muscle Repair, Cell 155(6) (2013) 1282-1295.
[10] L.C. Paredes, N. Olsen Saraiva Camara, T.T. Braga, Understanding the metabolic profile of macrophages during the regenerative process in zebrafish, Frontiers in Physiology 10(617) (2019).
[11] C.C. Bain, A. Schridde, Origin, Differentiation, and Function of Intestinal Macrophages, Frontiers in Immunology 9(2733) (2018).
[12] T. Wynn, A. Chawla, J. Pollard, Origins and hallmarks of macrophages: development, homeostasis, and disease, Nature 496 (2013) 445-455.
[13] T. Wynn, K. Vannella, Macrophages in tissue repair, regeneration, and fibrosis, Journal of Immunity 44 (2016) 450-462.
[14] I. Swinehart, S. Badylak, Extracellular matrix bioscaffolds in tissue remodeling and morphogenesis, Developmental Dynamics 245 (2016) 351-360.
[15] J. Godwin, A. Pinto, N. Rosenthal, Macrophages are required for adult salamander limb regeneration, Proceedings of the National Academy of Sciences of the United States of America 110 (2013) 9415-9420.
[16] Y. Luo, L. Shao, J. Chang, W. Feng, Y. Lucy Liu, M. Cottler-Fox, P. Emanuel, M. Hauer-Jensen, I. Bernstein, L. Liu, X. Chen, J. Zhou, P. Murray, D. Zhou, M1 and M2 macrophages differentially regulate hematopoietic stem cell self-renewal and ex vivo expansion, Blood Advances 2 (2018) 859-870.
[17] S. Jenkins, D. Ruckerl, P. Cook, L. Jones, F. Finkelman, N. van Rooijen, A. MacDonald, J. Allen, Local macrophage proliferation, rather than recruitment from the blood, is a signature of Th2 inflammation, Science 332 (2011) 1284-1288.

[18] M. Parmaksiz, A. Dogan, S. Odabas, A. Elçin, Y. Elçin, Clinical applications of decellularized extracellular matrices for tissue engineering and regenerative medicine, Biomedical Materials 11 (2016) 022003.
[19] K. Hussein, K.-M. Park, K.-S. Kang, H.-M. Woo, Biocompatibility evaluation of tissue-engineered decellularized scaffolds for biomedical application, Materials Science and Engineering: C 67 (2016) 766-778.
[20] L. Saldin, M. Cramer, S. Velankar, L. White, S. Badylak, Extracellular matrix hydrogels from decellularized tissues: structure and function, 49 (2017) 1-15.
[21] J. Aamodt, D. Grainger, Extracellular matrix-based biomaterial scaffolds and the host response, Biomaterials 86 (2016) 68-82.
[22] L. Huleihel, G.S. Hussey, J.D. Naranjo, L. Zhang, J.L. Dziki, N.J. Turner, D.B. Stolz, S.F. Badylak, Matrix-bound nanovesicles within ECM bioscaffolds, Science Advances 2(6) (2016) e1600502.
[23] L. Huleihel, J. Dziki, J. Bartolacci, T. Rausch, M. Scarritt, M. Cramer, T. Vorobyov, S. LoPresti, I. Swineheart, L. White, B. Brown, S. Badylak, Macrophage phenotype in response to ECM bioscaffolds, Seminars in Immunology 29 (2017) 2-13.
[24] S. Badylak, D. Freytes, T. Gilbert, Extracellular matrix as a biological scaffold material: structure and function, Acta Biomaterialia 5 (2009) 1-13.
[25] H. Engel, S. Kao, J. Larson, S. Uriel, B. Jiang, E. Brey, M. Cheng, Investigation of dermis-derived hydrogels for wound healing applications, Biomedical Journal 38 (2015) 58-64.
[26] M.-H. Cheng, S. Uriel, M. Moya, M. Francis-Sedlak, R. Wang, J.-J. Huang, S.-Y. Chang, E. Brey, Dermis-derived hydrogels support adipogenesis in vivo, Journal of Biomedical Materials Research: Part A 29A (2010) 852-858.
[27] S. Voytik-Harbin, A. Brightman, M. Kraine, B. Waisner, S. Badylak, Identification of extractable growth factors from small intestinal submucosa, Journal of Cellular Biochemistry 67 (1998) 478-491.
[28] S. Badylak, K. Kokini, B. Tullius, A. Simmons-Byrd, R. Morff, Morphologic study of small intestinal submucosa as a body wall repair device, Journal of Surgical Research 103 (2002) 190-202.
[29] B. Sicari, J. Dziki, B. Siu, C. Medberry, C. Dearth, S. Badylak, The promotion of a constructive macrophage phenotype by solubilized extracellular matrix, Biomaterials 35 (2014) 8605-8612.
[30] D. Freytes, R. Stoner, S. Badylak, Uniaxial and biaxial properties of terminally sterilized porcine urinary bladder matrix scaffolds, Journal of Biomedical Materials Research Part B: Applied Biomaterials 84B (2007) 408-414.
[31] D. Freytes, J. Martin, S. Velankar, A. Lee, S. Badylak, Preparation and rheological characterization of a gel form of the porcine urinary bladder matrix, Biomaterials 29 (2008) 1630-1637.
[32] B. Uygun, A. Soto-Gutierrez, H. Yagi, M.-L. Izamis, M. Guzzardi, C. Shulman, J. Milwid, N. Kobayashi, A. Tilles, F. Berthiaume, M. Hertl, Y. Nahmias, M. Yarmush, K. Uygun, Organ reengineering through development of a transplantable recellularized liver graft using decellularised liver matrix, Nature Medicine 16 (2010) 814-820.
[33] C. Deeken, A. White, S. Bachman, B. Ramshaw, D. Cleveland, T. Loy, S. Grant, Method of preparing a decellularised porcine tendon using tributyl phosphate, Journal of Biomedical Materials Research Part B: Applied Biomaterials 96B (2010) 199-206.

[34] M. Gerli, J. Guyette, D. Evangelista-Leite, B. Ghoshhajra, H. Ott, Perfusion decellularisation of a human limb: a novel platform for composite tissue engineering and reconstructive surgery, PLoS ONE (2018) 1-18.
[35] H. Geckil, F. Xu, X. Zhang, S. Moon, U. Demirci, Engineering hydrogels as extracellular matrix mimics, Nanomedicine 5 (2010) 469-484.
[36] M. Ciuffreda, G. Malpasso, C. Chokoza, D. Bezuidenhout, K. Goetsch, M. Mura, F. Pisano, N. Davies, M. Gnecchi, Synthetic extracellular matrix mimic hydrogel improves efficacy of mesenchymal stromal cell therapy for ischemic cardiomyopathy, Acta Biomaterialia 70 (2018) 71-83.
[37] S. Hinderer, S. Layland, K. Schenke-Layland, ECM and ECM-like materials — Biomaterials for applications in regenerative medicine and cancer therapy, Advanced Drug Delivery Reviews 97 (2016) 260-269.
[38] A. Altunbas, D. Pochan, Peptide-based and polypeptide-based hydrogels for drug delivery and tissue engineering, Topics in Current Chemistry 310 (2012) 135-167.
[39] A. Dasgupta, J. Mondal, D. Das, Peptide hydrogels, RSC Advances 3 (2013) 9117-9149.
[40] R. Xing, S.-Y. Li, N. Zhang, G. Shen, H. Möhwald, X. Yan, Self-assembled injectable peptide hydrogels capable of triggering antitumor immune response, Biomacromolecules 18 (2017) 3514-3523.
[41] D. Kumar, V. Workman, M. O'Brien, J. McLaren, L. White, K. Ragunath, F. Rose, A. Saiani, J. Gough, Peptide hydrogels—a tissue engineering strategy for the prevention of oesophageal strictures, Advanced Functional Materials 27 (2017) 1702424.
[42] E. Banwell, E. Abelardo, D. Adams, M. Birchall, A. Corrigan, A. Donald, M. Kirkland, L. Serpell, M. Butler, D. Woolfson, Rational design and application of responsive alpha-helical peptide hydrogels, Nature Materials 8 (2009) 596-600.
[43] N. Mehrban, B. Zhu, F. Tamagnini, F. Young, A. Wasmuth, K. Hudson, A. Thomson, M. Birchall, A. Randall, B. Song, D. Woolfson, Functionalized α-helical peptide hydrogels for neural tissue engineering, ACS Biomaterials Science & Engineering 1 (2015) 431-439.
[44] M. Rad-Malekshahi, L. Lempsink, M. Amidi, W. Hennink, E. Mastrobattista, Biomedical applications of self-assembling peptides, Bioconjugate Chemistry 27 (2016) 3-18.
[45] Y. Wu, J. Collier, α-Helical coiled-coil peptide materials for biomedical applications, Wiley Interdisciplinary Reviews: Nanomedicine and Nanobiotechnology 9 (2016) 1-17.
[46] S. Guven, P. Chen, F. Inci, S. Tasoglu, B. Erkmen, U. Demirci, Multiscale assembly for tissue engineering and regenerative medicine, Trends in Biotechnology 33 (2015) 269-279.
[47] S. Koutsopoulos, Self-assembling peptide nanofiber hydrogels in tissue engineering and regenerative medicine: progress, design guidelines, and applications, Journal of Biomedical Materials Research Part A 104 (2016) 1002-1016.
[48] R. Pugliese, M. Maleki, R. Zuckermann, F. Gelain, Self-assembling peptides cross-linked with genipin: resilient hydrogels and self-standing electrospun scaffolds for tissue engineering applications, Biomaterial Science 7 (2019) 76-91.
[49] N. Mehrban, E. Abelardo, A. Wasmuth, K. Hudson, L. Mullen, A. Thomson, M. Birchall, D. Woolfson, Assessing cellular response to functionalized α-helical peptide hydrogels, Advanced Healthcare Materials 3 (2014) 1387–1391.
[50] S. Badylak, G. Lantz, A. Coffey, L. Geddes, Small intestinal submucosa as a large diameter vascular graft in the dog, Journal of Surgical Research 47 (1989) 74-80.

[51] T. Gilbert, D. Stolz, F. Biancaniello, A. Simmons-Byrd, S. Badylak, Production and characterization of ECM powder: implications for tissue engineering applications, Biomaterials 26 (2005) 1431-1435.
[52] A. Massensini, H. Ghuman, L. Saldin, C. Medberry, T. Keane, F. Nicholls, S. Velankar, S. Badylak, M. Modo, Concentration-dependent rheological properties of ECM hydrogel for intracerebral delivery to a stroke cavity, Acta Biomaterialia 27 (2015) 116-130.
[53] A. BioMatrix, Kinetic Gel Stiffness (Rheology) of Varying Concentrations of Type I Collagen - FibriCol® 2019. https://www.advancedbiomatrix.com/wp-content/uploads/2016/03/Gel-Stiffness-Rheology-of-Type-I-Collagen-FibriCol-at-Various-Concentrations.pdf. (Accessed 23/08/2019 2019).
[54] R. Cleries, J. Galvez, M. Espino, J. Ribes, V. Nunes, M. de Heredia, BootstRatio: A web-based statistical analysis of fold-change in qPCR and RT-qPCR data using resampling methods, Computers in Biology and Medicine 42 (2012) 438-445.
[55] B. Sicari, N. Turner, S. Badylak, An In Vivo Model System for Evaluation of the Host Response to Biomaterials, in: R. Gourdie, T. Myers (Eds.), Wound Regeneration and Repair. Methods in Molecular Biology (Methods and Protocols), Humana Press, Totowa, NJ 2013, pp. 3-25.
[56] R. Fraioli, F. Rechenmacher, S. Neubauer, J. Manero, G. Javier, H. Kessler, C. Mas-Moruno, Mimicking bone extracellular matrix: integrin-binding peptidomimetics enhance osteoblast-like cells adhesion, proliferation, and differentiation on titanium, Colloids and Surfaces B: Biointerfaces 128 (2015) 191-200.
[57] M. Floren, W. Bonani, A. Dharmarajan, A. Motta, C. Migliaresi, W. Tan, Human mesenchymal stem cells cultured on silk hydrogels with variable stiffness and growth factor differentiate into mature smooth muscle cell phenotype, Acta Biomaterialia 31 (2016) 156-166.
[58] M. Haugh, T. Vaughan, C. Madl, R. Raftery, L. McNamara, F. O'Brien, S. Heilshorn, Investigating the interplay between substrate stiffness and ligand chemistry in directing mesenchymal stem cell differentiation within 3D macro-porous substrates, Biomaterials 171 (2018) 23-33.
[59] T. Dorsey, D. Kim, A. Grath, D. James, G. Dai, Multivalent biomaterial platform to control the distinct arterial venous differentiation of pluripotent stem cells, Biomaterials 185 (2018) 1-12.
[60] J. Dziki, D. Wang, C. Pineda, B. Sicari, T. Rausch, S. Badylak, Solubilized extracellular matrix bioscaffolds derived from diverse source tissues differentially influence macrophage phenotype, Journal of Biomedical Materials Research Part A 105 (2017) 138-147.
[61] A. Huber, A. Boruch, A. Nieponice, H. Jiang, C. Medberry, S. Badylak, Histopathologic host response to polypropylene-based surgical mesh
materials in a rat abdominal wall defect model, Journal of Biomedical Materials Research Part B: Applied Biomaterials 100B (2011) 709-717.
[62] D. Faulk, R. Londono, M. Wolf, C. Ranallo, C. Carruthers, J. Wildemann, C. Dearth, S. Badylak, ECM hydrogel coating mitigates the chronic inflammatory response to polypropylene mesh, Biomaterials 35(30) (2014) 8585-8595.
[63] A. Blakney, M. Swartzlander, S. Bryant, The effects of substrate stiffness on the in vitro activation of macrophages and in vivo host response to poly(ethylene glycol)-based hydrogels, Journal of Biomedical Materials Research: Part A 100 (2012) 1375-1386.

[64] R. Sridharan, A. Cameron, D. Kelly, C. Kearney, F. O'Brien, Biomaterial based modulation of macrophage polarization: a review and suggested design principles, Materials Today 18 (2015) 313-325.
[65] E. White, A. Mantovani, Inflammation, wound repair, and fibrosis: reassessing the spectrum of tissue injury and resolution, Journal of Pathology 229 (2013) 141-144.
[66] C. Du, Y.-Q. Jin, J.-J. Qi, Z.-X. Ji, S.-Y. Li, G.-S. An, H.-T. Jia, J.-H. Ni, Effects of Myogenin on expression of late muscle genes through MyoD-dependent chromatin remodelling ability of Myogenin, Molecules and Cells 34 (2012) 133-142.
[67] J. Tidball, S. Villalta, Regulatory interactions between muscle and the immune system during muscle regeneration, American Journal of Physiology: Regulatory, Integrative and Comparative Physiology 298 (2010) R1173-R1187.
[68] D. Discher, D. Mooney, P. Zandstra, Growth factors, matrices, and forces combine and control stem cells, Science 324 (2009) 1673-1677.
[69] B. Brown, B. Sicari, S. Badylak, Rethinking regenerative medicine: a macrophage centered approach, Frontiers in Immunology 5 (2014) 1-11.